Cement & Concrete Composites 36 (2013) 48–55

Contents lists available at SciVerse ScienceDirect

Cement & Concrete Composites

journal homepage: www.elsevier.com/locate/cemconcomp

Atomic force and lateral force microscopy (AFM and LFM) examinations of cement and cement hydration products

A. Peled [a,*], J. Castro [b], W.J. Weiss [c]

[a] Structural Engineering Department, Ben Gurion University of the Negev, Beer Sheva, Israel
[b] School of Engineering, Pontificia Universidad Catolica de Chile, Santiago, Chile
[c] School of Civil Engineering, Purdue University, West Lafayette, IN, USA

ARTICLE INFO

Article history:
Received 31 January 2012
Received in revised form 20 August 2012
Accepted 22 August 2012
Available online 11 September 2012

Keywords:
Atomic force microscope (AFM)
Lateral force microscope (LFM)
Cement
Mortar
Cement hydrates
Nanostructure
Interfacial transition zone (ITZ)

ABSTRACT

The objective of this work was to better understand how atomic force microscopy (AFM) and lateral force microscopy (LFM) techniques can be used as tools to understand the nanostructure and microstructure of cement and cement hydration products. AFM and LFM techniques were used on mortar samples to distinguish between CSH, CH, and unhydrated cement particles. The LFM technique appears to be more sensitive to topographic changes than conventional AFM and it can more clearly distinguish between the different phases at high magnification (low scan range). AFM could also be used to calculate the roughness of the interfacial transition zone (ITZ) between aggregate and the cement paste at different ages. The rough surface at the interface of the paste and aggregate is generally interpreted as higher porosity. It was found that a reduction in roughness (i.e., porosity) occurred for samples that were cured for a longer time which are consistent with the explanation of porosity.

1. Introduction

Cement-based materials are composed of amorphous phases, crystalline phases, water, and a wide range of pore sizes and shapes. Calcium-silicate-hydrate (CSH) is the dominant product of the hydration process, forming up to 60% of the hydrated cement paste volume. Calcium hydroxide crystals (CH) make up approximately 25% of the volume of the paste [1]. When aggregates are added to the paste the interfacial transition zone (ITZ) between aggregate and paste also influences the structure of the system on the nano and microscales. Since the nanoscale features are related to the performance and behavior of the material at the macro scale, resolving their structure at the nanoscale is helpful for understanding the behavior of hardened cement paste, mortar, and concrete.

Scanning electron microscopy (SEM) is used extensively to investigate the structure of cement-based materials at the microscale. Recently there is a growing interest to use scanning probe microscopes (SPMs) to study the micro and nanostructural characteristics of hardened cement-based materials. One of the methods that has recently been explored is the use of depth sensing micro-indentation for characterization elastic and fracture characteristics including its hardness, stiffness, and toughness [2–6]. Recently, atomic force microscopes (AFMs) have been used for the purpose of nanoindentation to determine mechanical characteristics at the nanoscale of cementitious materials (i.e., mainly the CSH phase) [5,7,8]. The AFM provides accurate positioning capabilities while offering a three dimensional image of the indentation impression. However indentation from AFM is typically performed at lower force levels than other indentation methods. Little work was done using AFM to characterize the micro and nanostructures including detailed morphology characteristics including the shape and size of features at the nanoscale of harden cement paste, mortar and concrete.

Atomic force microscopy (AFM) is a high resolution scanning probe microscope that can provide a topographical representation of a sample surface. Topographic images are obtained using a probe with a sharp tip at the end of cantilever. The tip of the cantilever is moved across the surface of a specimen. As this tip is brought into contact with the surface of the specimen the deflection of the tip can be measured and the topography of the surface is recorded [9]. By using this technique, AFM can provide detailed surface texture characteristics on particle shape for harden cement systems at a scale that cannot be provided by SEM [10–12]. Papadakis and Pedersen [10] found sufficient correlation between microscopic quantitative information provided by the AFM with

* Corresponding author. Tel.: +972 8 6479672; fax: +972 8 6479670.
E-mail address: alvpeled@bgu.ac.il (A. Peled).

0958-9465/$ - see front matter © 2012 Elsevier Ltd. All rights reserved.
http://dx.doi.org/10.1016/j.cemconcomp.2012.08.021

macroscopic mechanical and durability parameters associated with cementitious products. Yang et al. [11,12] studied the surface structure of cement paste in humid air by AFM and noticed that the structure changes from coarse to fine grains as the humidity is changed.

Lateral force microscopy (LFM) is a derivative of AFM. In LFM the tip is maintained in contact with the sample surface and the 'twisting of the cantilever' is measured in addition to the vertical deflection (i.e., the approach that is more common for AFM). The detector on the cantilever arm collects a lateral deflection signal from the cantilever's twisting motion when it is used for LFM. The strength of the lateral deflection signal is related to the frictional force between the sample surface and the tip. Therefore the lateral deflection can be related to the friction of the surface. The LFM method is more sensitive to topographical variations than other methods. Until recently very little work has been reported on using the LFM technique to characterize the micro and nanostructures of harden cement-based materials.

The objective of this work was to understand how AFM and LFM techniques can be used as tools to provide insights on the structure of cement and cement hydration products. Mortar samples were prepared for this study. Two approaches were taken in the investigations using AFM and LFM. The first approach focused on investigating surface texture characteristics of hardened cement paste components such as CSH, CH and unhydrated cement particles using detailed images. The second approach focused on studying topographic differences at the aggregate cement paste interface (i.e., at the interfacial transition zone (ITZ)) due to different curing conditions. SEM and energy dispersive X-ray (EDX) were used to select appropriate regions for the AFM/LFM study to provide background information on the obtained images and surface characteristics.

2. Experimental study

2.1. Sample preparation

Mortar samples were prepared with a w/c (water to cement ratio) of 0.30 and 55% volume of natural fine aggregate (details are provided in Table 1 and Ref. [13]). The mortar samples were cast, sealed, and placed in an environmental chamber at 23 ± 1 °C until the samples reached an age of 1, 7 and 28 days. At each age of testing, the specimens were demolded and cut using a diamond tipped wafer saw with a low viscosity mineral oil as the coolant/lubricant. The mineral oil also helped to minimize additional hydration. The mortar slices were then immersed in acetone to remove the remaining free water and oil. After drying for several hours at room temperature the mortar slices were placed in a vacuum chamber for approximately 24 h and then placed in an oven at 50 °C for at least 3 days. The drying and oven conditioning steps were performed in an effort to remove the remaining free water from the pores to cease the hydration process. This was most important for the early age samples (i.e., the samples prepared at an age of 1 and 7 days).

After drying, the samples were ground with successive wheels of increasingly fine diamond paste (up to 0.25 μm) using low viscosity mineral oil (more details are provided in Refs. [13,14]). The polishing process was based on the method developed by Diamond [15]. The specimens were polished (without epoxy impregnation as the epoxy may penetrate into the cement paste pores, influencing the topographic characteristics measured by the AFM and even more by the LFM). To expose an un-carbonated area for investigation, the polished samples were cut into slices approximately 5 mm tall as required for positioning in the AFM, then cleaned in an ultrasonic acetone bath and stored in an oven at 50 ± 2 °C for several days until used under the AFM/LFM and SEM.

Table 1
Mixture proportions (in SSD).

Material	Proportions
Volume fraction of aggregates, %	55
w/c, by mass	0.3
Cement (kg/m^3)	727.0
Water (kg/m^3)	218.1
Aggregate (kg/m^3) SSD	1442.0
WRA (g/100 g cement)	0.6

2.2. AFM–LFM

The atomic force microscope used in this study was a Digital Instruments CP-II AFM system (manufactured by Veeco) with a silicon tip and a cantilever arm having the following dimensions: *T*: 3.5–4.5 μm, *L*: 515–535 μm and *W*: 30–40 μm, with a resonance frequency of 19–24 kHz, and 0.9 N/m spring constant. The microscope was operated in contact mode to provide topographic maps of the cement paste and mortar surfaces with a set point of 180 nN and scan speed of 0.5 Hz, using both AFM and LFM techniques. The tips were replaced frequently during scanning to avoid blunting while keeping high scanning resolution. During scanning the specimen was at room conditions (23 ± 2%, 45 ± 7% RH).

Different scan ranges of 50 μm, 15 μm, 10 μm and 3 μm and 1 μm were used in order to better understand the surface structure and particle shapes. The results shown in this paper consist of typical results obtained from these scans.

The regions used in the ITZ examination were selected after first using the optical microscope connected to the AFM to find the most interesting regions. Similarly, the region that was selected to study the hardened cement paste features was selected after performing SEM and EDX analysis as explained in the following section.

2.3. SEM–EDX

The scanning electron microscope (SEM) used in this study was a RJ Lee personal scanning electron microscope. The SEM was used in backscattered (B) mode with high vacuum condition to select the region to be scanned under the AFM. The goal was to select a typical zone of cement paste containing several features such as calcium hydroxide (CH), calcium silicate hydrates (CSH), and an un-hydrated cement particle. Energy dispersive X-ray (EDX) analysis was carried out to distinguish between the different features of the selected regions. The polished specimens were coated with a thin layer of palladium in order to observe these elements under the SEM. After the SEM observations and EDX analysis were performed, the coating was removed using acetone and the same specimen was immediately scanned using the AFM at the regions identified by the SEM and EDX. This was done to study the harden cement paste component characteristics.

3. Results and discussion

3.1. SEM–EDX

SEM BS observations were conducted on the entire surface area of the polished specimen to search for a region of the cement paste that can be scanned under the AFM and LFM. While numerous samples were examined, a typical region for a sample that was cured for 28 days is presented in Fig. 1a. This area was chosen to be scanned using the AFM and LFM as it contains several elements

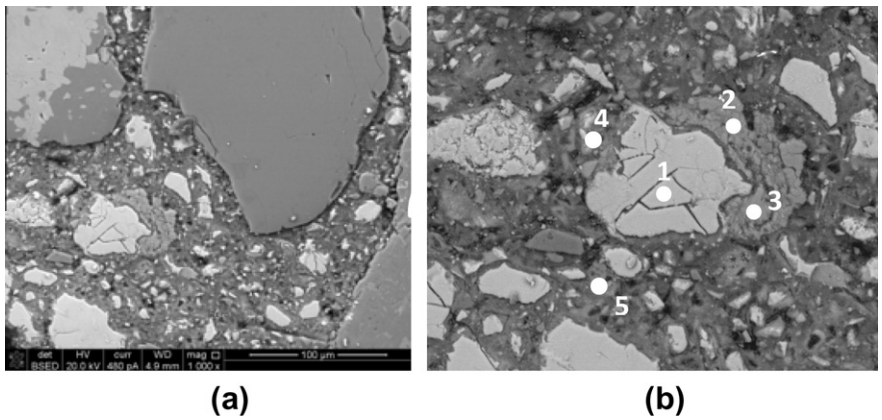

Fig. 1. SEM BS images: (a) entire observed area, and (b) scanned area of different elements (presented by a point with a number); un-hydrated cement particle – Spectrum 1, CH – Spectrums 2 and 3, and CSH – Spectrums 4 and 5.

within the cement paste region: unhydrated cement particles – the elements in white, CH located around one of the unhydrated cement particle having light gray color, and CSH phase – the darker gray particle in the figure. Higher magnification of this region was conducted using SEM BS mode and is presented in Fig. 1b, highlighting the different elements within the cement paste zone. The scanning direction that was used with the AFM was along the width of the image in Fig. 1b, i.e., from left to right and vice versa.

Five different locations were selected for investigation based on the results of energy dispersive X-ray (EDX). The selected regions included one unhydrated particle location (labeled 1 in Fig. 1b), two CH locations (labeled 2 and 3 in Fig. 1b) and two CSH locations (labeled 4 and 5 in Fig. 1b). EDX results can clearly identify the element composition at each region. EDX results from point 1 (Fig. 1b) indicates an unhydrated cement particle due to the high content of calcium and silica (Ca = 53.3, Si = 12.5, and O = 34.2). The EDX results of the second and third points (2 and 3 in Fig. 1b) identify calcium hydroxide as calcium and oxygen are observed (Ca = 47.3, O = 50.0, with hardly any silica Si = 2.7). The EDX results of the forth and five spots (4 and 5 in Fig. 1b) indicate a CSH phase where silica and calcium are both present (Si = 11.5, Ca = 48.3, and O = 40.2).

3.2. AFM–LFM comparison

3.2.1. Overview

AFM and LFM techniques were used to provide topographic maps of the selected regions (cured for 28 day), focusing on the CSH and CH phases. The color scale for the AFM images represents differences in topography (i.e., surface heights), with darker colors corresponding to lower surface height and a lighter color corresponding to a higher surface height. For LFM, different colors represent differences in mean voltage which represent the cantilever's twisting motion, and can be related to the friction force of the surface. The darker color corresponds to a lower voltage and smaller friction forces as lighter colors correspond to a higher voltage and greater friction forces.

Fig. 2 shows AFM and LFM images of the same area observed by SEM, discussed above (Fig. 1b) including the unhydrated particle and the CH and CSH phases. The AFM (Fig. 2a) and the LFM (Fig. 2b) images are of exactly same scanned region. The different features of the unhydrated particle, CSH and CH are clearly observed by the AFM technique. For the LFM, the different features are identified but not as clearly as by the AFM, the hardened cement paste looks fairly flat and smooth with not as significant difference between the various components and their textures.

3.2.2. CH phase

Two represented locations at the CH phase (as identified by the EDX) were closely scanned (at the white dotted squares in Fig. 2a) using the AFM and the LFM techniques with a scan range of 3 μm (Fig. 3). This was in order to explore the surface texture characteristics of the CH phase. Also here the AFM and the LFM images are of exactly same scanned region, at the two zones. Both techniques, AFM and LFM, show that the CH phase is composed from clusters of small grains with sizes of several dozen nm. The granular structure is observed in both scanned regions with the two measurement methods AFM (Fig. 3a and c) and LFM (Fig. 3b and d); however the morphology structure and the grains are much clearer with better separation when using the LFM technique. This means that in the case of high magnification (low scan range) the LFM is beneficial in providing more detailed images as compared with the AFM technique; however for low magnification (larger scale) the AFM offers an advantage (Fig. 2).

As mentioned the AFM represents differences in surface heights therefore when there is a relatively large difference in heights in the scan region it is easier to capture features that are higher surfaces, and much harder to capture features that are at the lower surfaces (i.e., some texture information can be missing as observed in the dark areas in Fig. 3a and c). Following this interpretation, it is easier to recognize the upper surface of a feature then the whole topographic of this component, when using the AFM. These are most significant for high resolution (low scale ranges). On the other hand, LFM images represent differences in voltage which represent the twisting motion of the cantilever, i.e., lateral movement known to be related to frictional resistance, but can also be due to different heights, therefore showing more clearly topographical variations mainly at low scan range (high magnification). In the case of hardened cement paste, due to its heterogenic characteristic, polishing is challenging. As a result it appears that the LFM is suited better to capture different features, mainly at high resolution (i.e., low range of scanning), providing detailed structural information.

When observing the LFM and AFM images at high resolution (Fig. 3), it is also interesting to note that although both scanned regions represent the CH phase (as identified by the EDX), the surface morphology is quite different between the two regions (Fig. 3a–d). In one (Fig. 3b), hexagonal crystal morphology at a range of 1 μm is clear with the LFM. In this spot the CH crystals are lying on top of the other, suggesting a layered structure which is consistent with previous observations and representing the CH structure. When observing the AFM image at this spot (Fig. 3a) such crystal structures are not as clear. It appears that each hexagonal unit is

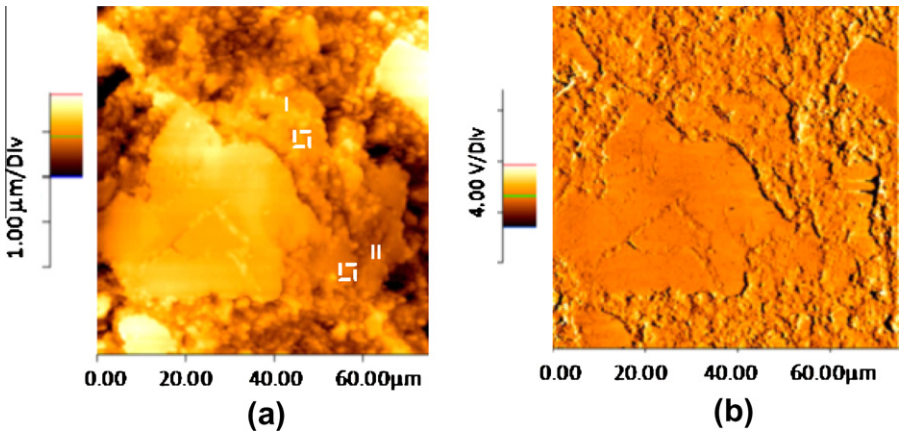

Fig. 2. An overview observation, same zone as the SEM image in Fig. 1b using the: (a) AFM, and (b) LFM techniques.

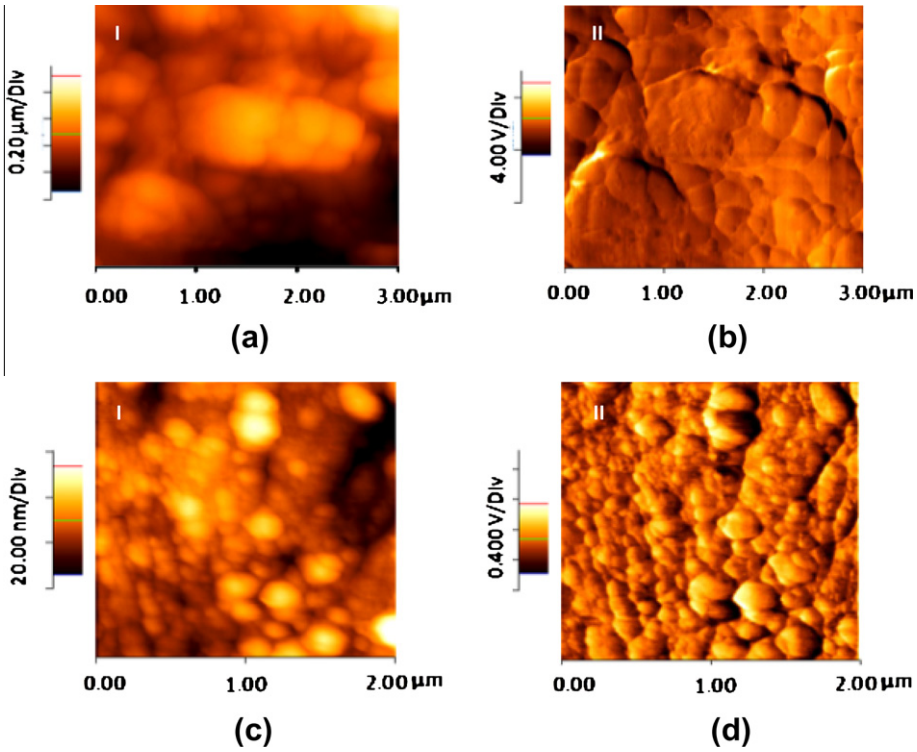

Fig. 3. The CH phase at two different regions I and II (labeled in Fig. 2a) using: (a and c) the AFM, and (b and d) the LFM techniques.

composed of smaller units. These small units are seen in both AFM and LFM images but are much more clear and separate in the case of the LFM. At the other region (Fig. 3c and d) the clear crystals are observed but many small and clear grains are recognized, providing a rough granulated structure. Also, in this region some clusters of grains are seen but not with as clear crystal geometry as the previously discussed region. Also within this scanned zone the grainy texture is better pronounced and clear when using the LFM technique. It should be noted that the sample was scanned at room environment where scanning could last several hours, thus some of the morphology observed may be due to carbonation.

3.2.3. CSH phase

The images present in Fig. 4a and d show LFM and AFM topographic maps of the square dots area in Fig. 1b. This region includes both zones that of CH and that of CSH at a scan range of 15 µm. The CSH phase was investigated in more detailed at the zone near the CH phase (presented by the dotted square in Fig. 4a and d). It is observed that the CSH phase is composed of clusters of grains which are not observed at the CH phase at this scan range. Higher magnification on the CSH region, of 3 µm scan range, clearly shows this granular structure (Fig. 4b and e). Grains with sizes in the range of hundreds of nanometers are observed (Fig. 4c and f). Images of single CSH grain clearly show a CSH grain with a size of 530×710 nm (Fig. 4c) and 273×476 nm (Fig. 5a). Such a structure of the CSH is comparable with the description of Type III CSH phase as by Diamond [16]. The structure is observed in both AFM (Fig. 4a–c) and LFM (Fig. 4d–f) measurements; however these grains are much clearer with better separation when using the LFM technique, similar to the observations of the CH phase discussed above. Note that similar structure of the CSH presented here was also observed at Spectrum 5 in Fig. 1b (identified by EDX, see

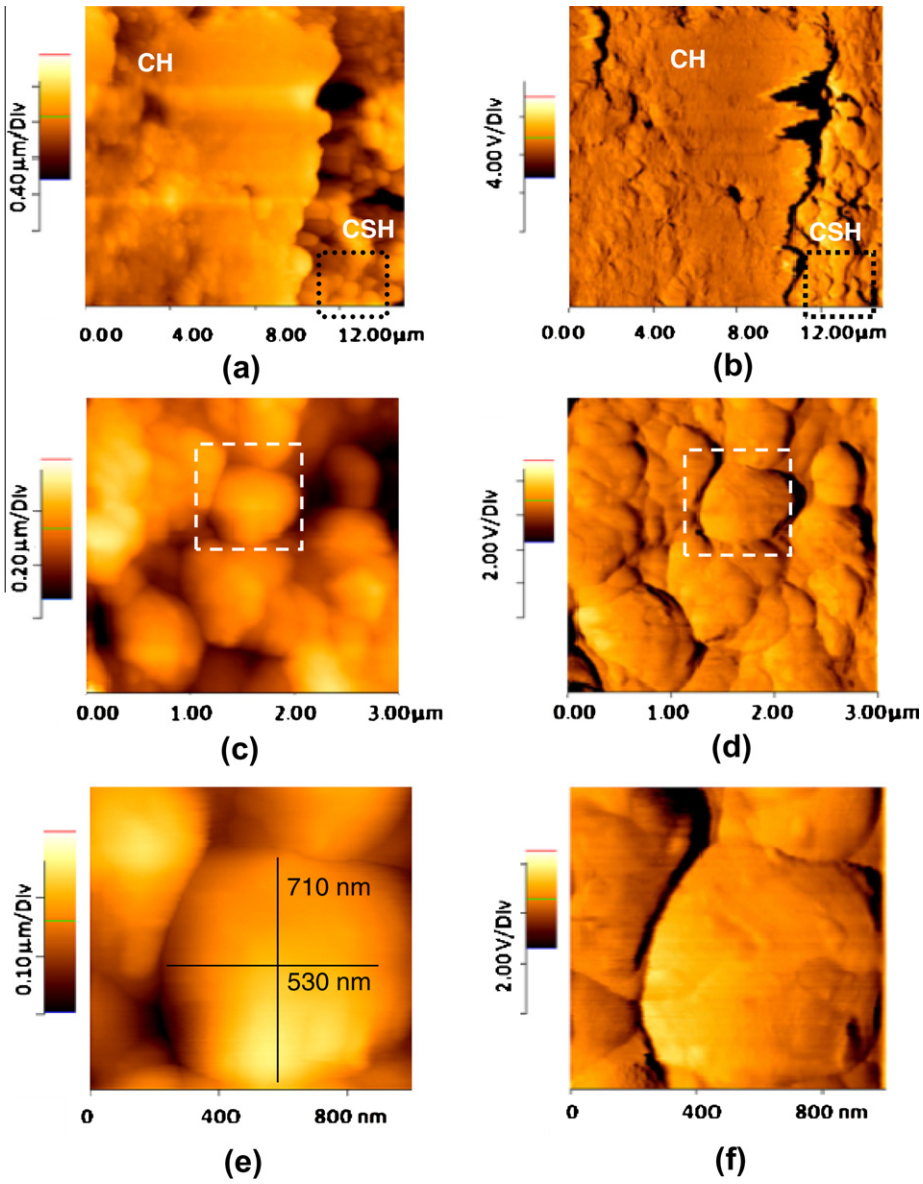

Fig. 4. Images taken by: (a, c, and e) AFM, (b, d, and f) LFM at different scan ranges. (a and b) Observing CH and CSH phases, (c and d) focusing on the CSH phase at the square dotted region in (a) and (b), (e and f) detailed images on CSH grain presented by the square dotted in (c) and (d).

Ref. [14]) which supports the observations here. This particulate nature of the CSH is also observed under the SEM at high magnification (60 K, Fig. 5b), but with not as clear and detailed texture observed by the LFM method.

LFM also allows identifying closer detailed textures and tiny features on top of the grain surface to be identified (Fig. 6b) at high magnification, which is not seen by the AFM (Fig. 6a). Here a thin coating layer is seen by the LFM technique only, partly covering the grains cluster surface. Assemblies of several grains are observed when looking at the LFM image as some particles are partly coated but still clear. This type of information is unique to the LFM technique, as the thin coating layer is not observed at all with the AFM technique. Moreover, it is hard to recognize the assembled grains when employing the AFM technique. These images again show the benefit of the LFM to provide tiny detailed structural features as compared to much less texture information obtained by the AFM, at high magnification (low scan range).

3.2.4. Comparison of CH–CSH phases

Figs. 4a, b and 7 present scanned regions that include both CH and CSH phases (this scan region is the square dots in Fig. 1b), using both the AFM and LFM methods. In these images the two phases of the cement paste were scanned together with the exact same environmental conditions. The same area was scanned twice in two different ranges, the first scan range was 15 µm (Fig. 4a and b), i.e., at relatively large scan range and the second scan range was at a smaller range of 3 µm. At the higher scan range (Fig. 4d) it is highly noticeable that the CH region is flat and smooth and no grain structure is observed. On the other hand, the CSH area is relatively rough with a grainy structure as discussed above. These observations are made using both scan techniques (LFM and AFM). This combined scan image clearly illustrates the difference in the structure of these two cement paste products. When comparing the two phases at the lower scan range (higher magnification, Fig. 7) the differences can be seen. The CSH is rough, bumpy

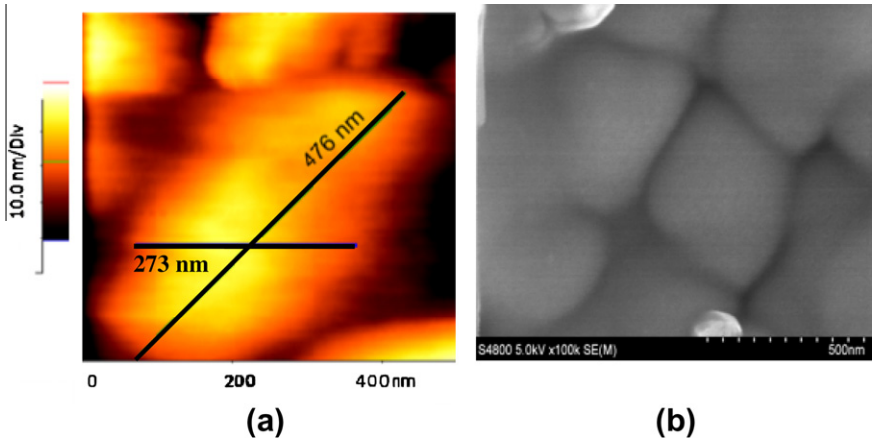

Fig. 5. (a) Single CSH grain at 1 μm scale range, and (b) observation on CSH by SEM (×60 K).

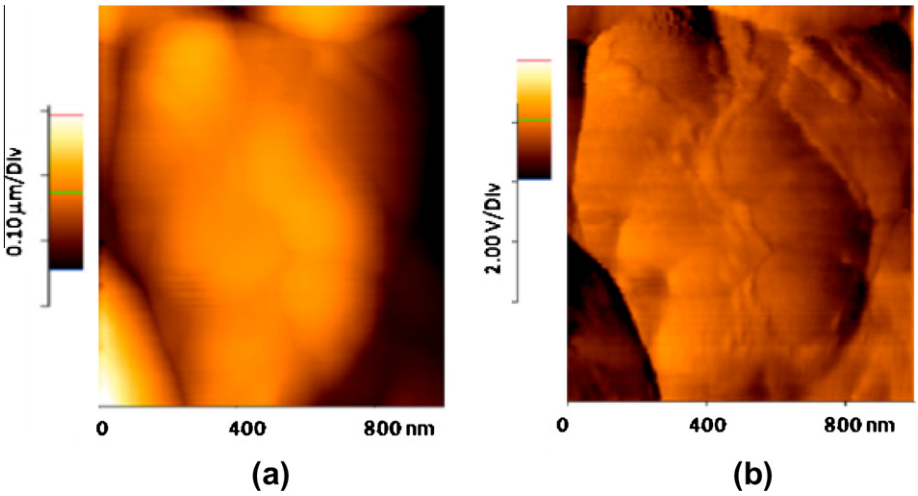

Fig. 6. Detailed images on CSH phase using: (a) AFM) and (b) LFM techniques.

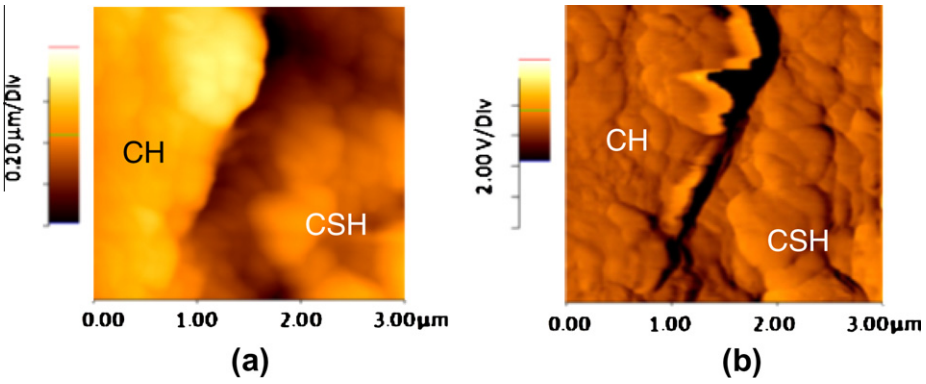

Fig. 7. Images including both regions of CH and CSH products (the dotted square area in Fig. 1b) taken by: (a) AFM, and (b) LFM at 3 μm scan range.

and grainy at the surface of the CSH which is in contrast to the smoother surface of the CH region. Again these were observed by both methods AFM and LFM. However at this scan range when using the LFM, the surface of the CH also shows some particle based structure but at much smaller range. This particulate structure is not observed by the AFM which showing a relatively smooth and flat surface at the CH phase zone at such high magnification. This indicates that in both regions, the CSH and CH are assemblies but they are at different range, structure and size. Based on the finding of this study the CSH particles are in the range of hundreds nanometers (Figs. 5a and 4e), whereas the CH grains are in the range of dozen nm. The comparison of the AFM and LFM images again shows the benefit of using LFM for obtaining detailed texture features of hardened cement paste.

It should be noted that the scanning was done at ambient air condition and therefore moisture and carbonation are possible on the scan area as well as in between the tip and substrate which can influence the information collected at the scanned surface [9].

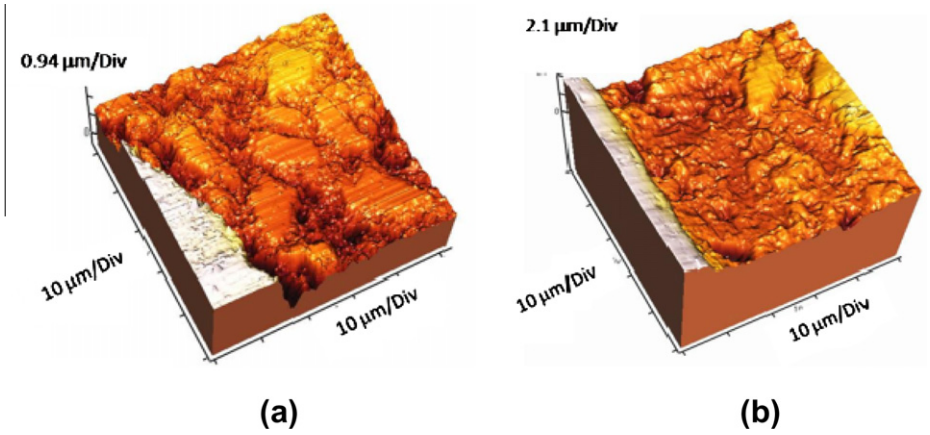

Fig. 8. 3D AFM images at different curing ages: (a) 2 day, and (b) 28 day.

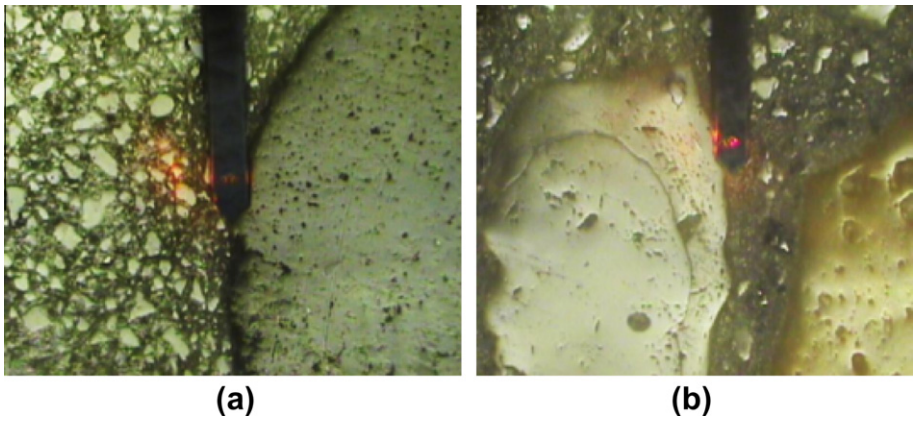

Fig. 9. Observations on ITZ of mortars at (a) 1 day and (b) 28 day of curing, by optical microscope connected to the AFM (including the tip of the AFM).

3.3. Influence of curing

Mortar samples were prepared and evaluated at different curing ages, 1 day, 7 day and 28 day. AFM images of the different curing ages were compared and analyzed, to see whether the AFM technique enable to distinguish between several aged systems in order to farther learn the potential abilities of these nanotechnology methods.

A comparison of the AFM images (3D) taken at ages of 1 day and 28 day are presented in Fig. 8. The figure demonstrates images at 50 µm scale near an aggregate. It can be noticed that the white area (at the side of the images) represents the aggregate and the darker areas are related to the pores. Relatively large un-hydrated cement grains of about 25 µm are clearly observed at 1 day (Fig. 8a), however no such large particles are observed after 28 day (Fig. 8b). These observations correlate well with the optical images taken during scanning by the AFM (Fig. 9). Also, with the optical microscope observations, fewer unhydrated particles are observed after 28 day of curing as compared to 1 day of curing. Moreover, a relatively smooth surface is measured in the paste at the interface of the 28 day old specimen while a much rougher surface is observed for the 1 day old sample when observing the 3D AFM images (Fig. 8). This observed trend implies greater porosity and lower hydration at 1 day curing versus greater hydration and denser ITZ after 28 day of curing, as one may expect [17].

To compare these systems using a more quantitative analysis the roughness of each image was calculated. A minimum of 10 scans were performed for each specimen with a 50 µm scan range, in which about 40 µm were mapped the cement paste (the rest was the aggregate).

The scanned topographic images were analyzed using the DiProScan data acquisition software. The region of the cement paste only (without the aggregate) was analyzed for all aged systems. The average roughness of each image was calculated using following equation:

$$R_{ave} = \sum_{n=1}^{N} \frac{|z_n - z_m|}{N} \quad (1)$$

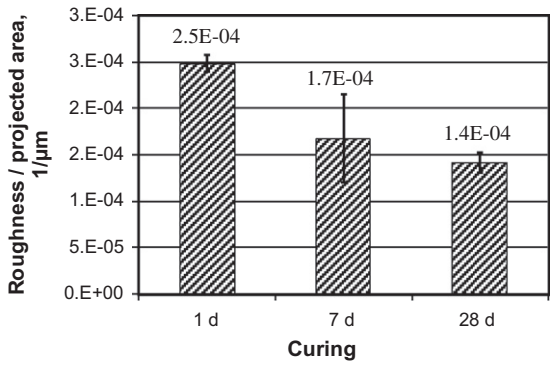

Fig. 10. Roughness results at the ITZ of mortars of different curing duration, based on 3D AFM images.

where Z_m is the mean Z height. The average roughness refers only to the analyzed areas (excluding the aggregate), with N given by the number of data points in the included area.

The assumption was that a sample with a higher surface roughness implies that the specimen has a higher porosity. Also, the projected surface of the scan area of each analysis region was calculated. The projected area is the area of the paste without the aggregate (projected area $= L \times w$ where L is the length of the selected region to analyzed and w is the width of this selected region). The average roughness value was normalized by the projected area in order to enable comparison between the different tested systems.

Fig. 10 presents the normalized roughness values for the three different curing systems. A reduction in roughness is observed as the curing period increased. This means that at later age the harden cement paste is less porous due to hydration. The effect of curing on the cement paste density and the reduction in unhydrated particles content during aging is well known and expected.

These results may indicate the ability of using AFM topographic images to identify porosity, hydration products and other characteristics related to the ITZ of mortar and hardened cement paste at the nanoscale.

4. Conclusions and summary

In this paper atomic force microscopy (AFM) and lateral force microscopy (LFM) were used as tools to examine hardened cement paste and the ITZ of mortars. First, AFM and LFM were used to interrogate different phases of hydrated cement paste: CSH particles, CH crystals and unhydrated cement particles at the nano and microscale. Second, the structure of ITZ in the mortars was interrogated after 1, 7 and 28 day.

At high scan range (low magnification) AFM could more clearly distinguish between the features of the unhydrated cement particle, CSH and CH, as compared with LFM where the different features were not identified as clearly. On the other hand, at low scan range (high magnification) LFM was found to be more sensitive to topographic changes and could provide more detailed texture features of the hardened cement paste. LFM is suited better to capture different features, mainly at high resolution (i.e., low range of scanning), whereas at low magnification (larger scale) the AFM offers an advantage.

Both measurements, AFM and LFM methods, could distinguish between the two cement paste products: CSH and CH. When comparing the CSH and CH regions at large magnification of ~15 μm and above, rough, bumpy and grainy structure was observed at the surface of the CSH and much smoother surface with no grain structure was observed at the CH region. This clearly illustrates the difference in the structure of these two cement paste products.

At low scan ranges (~3 μm and lower):

- The CSH phase was found to be composed of clusters of grains, as at the low scale, with sizes in the range of hundreds of nanometers. The structure was observed in both AFM and LFM measurements; however these grains were much clearer with better separation when using the LFM technique. These observations of the CSH structure were supported by SEM at high magnification (60 K), but with not as clear and detailed texture as observed by the LFM method.
- The CH phase at this low scale range found to be composed from particle based structure as the CSH, indicating a rough granulated structure also of this phase but with smaller grain sizes of several dozen nm. Also within this scanned zone the grainy texture was more pronounced and clear when using the LFM technique. In some cases hexagonal crystal morphology at a range of 1 μm lying on top of the other was clearly recognized with the LFM only, where each hexagonal unit was composed of smaller cluster units. This suggests a layered structure which is consistent with previous observations and representations of the CH structure.

These observations clearly illustrate the difference in the morphology of the CSH and CH cement paste products; both are assemblies but with different range, structure and size, when using the LFM and AFM methods.

The LFM could also provide unique information identifying tiny features on top of the grain surface, such as a thin layer partly covering the grains cluster surface. This type of information was not observed at all with the AFM technique. This indicates again the benefit of the LFM to provide tiny detailed structural features as compared to much less texture information obtained by the AFM, at high magnification (low scan range).

Three dimensional AFM images were compared for samples that were different ages. The roughness of the imaged regions was calculated, assuming that higher roughness was related to greater porosity. It was found that the roughness (i.e., porosity) of the mortar at the interface of the paste and aggregate reduced as the sample aged. These results highlight the ability to use the AFM technique to identify structure differences of mortars.

References

[1] Mindess S, Young JF, Darwin D. Concrete. 2nd ed. NJ: Prentice Hall; 2003.
[2] Nemecek J, Kopecky L, Bitnar Z. Nanoindentation size effect of cement pastes: nanotechnolgy in construction 2. In: Proceedings second international symposium. Nanotechnolgy in Construction, vol. 37; 2005. p. 161–8.
[3] Sonebi M. Utilization of depth-sensing micro-indentation technique to determine the micromechanical properties of ITZ in cementitious materials. In: Proceedings on nanotechnology of concrete: recent developments and future perspectives. ACI SP-254; 2008. p. 57–68.
[4] Zhu W, Sonebi M, Bartos PJM. Bond and interfacial properties of reinforcement in self-compacting concrete. Mater Struct 2004;37:442–8.
[5] Mondal P, Shah, SP, Marks LD. Use of atomic force microscope and nanoindentation for characterisation of cementitious materials at the nanoscale. In: Proceedings on nanotechnology of concrete: recent developments and future perspectives. ACI SP-254; 2008. p. 41–9.
[6] Fisher-Cripps AC. Nanoindentation. 2nd ed. New York: Springer Verlag; 2004.
[7] Reda Taha MM, Al-Haik M, Adam I, Tahrani M, Reinhardt A. Nano versus macro creep compliance of concrete. In Tanabe et al., editors. Proceedings of creep, shrinkage and durability mechanics of concrete and concrete structures. CONCREEP 08. 1; 2008. p. 229–35.
[8] Ibarra YS, Gaitero JJ, Erkizia E, Campillo I. Atomic force microscopy and nanoindentation of cement pastes with nanotubes dispersion. Phys State Solut (a) 2006;203(6):1076–81.
[9] Butt H-J, Cappella B, Kappl M. Force measurements with the atomic force microscope: technique, interpretation and applications. Surf Sci Rep 2005;59:1–15.
[10] Papadakis VG, Pedersen EJ. An AFM-SEM investigation of the effect of silica fume and fly ash on cement paste microstructure. J Mater Sci 1999;34:683–90.
[11] Yang T, Keller B, Magyari E. AFM investigation of cement paste in humid air at different relative humidities. J Phys D Appl Phys 2002;35(8):L25–8.
[12] Yang T, Keller B, Magyari E. Direct observation of the carbonation process on the surface of calcium hydroxide crystals in hardened cement paste using an atomic force microscope. J Mater Sci 2003;38:1909–16.
[13] Peled A, Castro J, Weiss J. Atomic force microscope examinations of mortar made using water-filled lightweight aggregate. Transportation Research Record: Journal of the Transport Research Board. Washington, DC: Transportation Research Board of the National Academies; 2009;2141:92–101.
[14] Peled A, Weiss J. Hydrated cement paste constituents observed with atomic force and lateral force microscopy. Constr Build Mater J 2011;25(1):4299–302.
[15] Diamond S. The microstructure of cement paste and concrete—a visual primer. Cem Concr Compos 2004;26:919–33.
[16] Diamond S. Hydraulic cement pastes: their structure and properties. In: Proceedings of conference. Tapton Hall 2; 1976.
[17] Zampini D, Shah SP, Jennings HM. Early age microstructure of the paste–aggregate interface and its evolution. J Mater Res 1998;13(7):1888–98.